Thunderstorm high frequency radio bursts with weak low frequency radiation

Ningyu Liu[1] and Joseph R Dwyer[2]

[1]The University of New Hampshire
[2]University of New Hampshire

November 24, 2022

Abstract

Brief bursts of high frequency (HF) and very high frequency (VHF) radio emissions unaccompanied by strong low frequency radiation have been observed during initiation and propagation of lightning or thunderstorm electrical breakdown without leading to fully-fledged lightning. This paper investigates a physical mechanism to generate such radio bursts by electrical discharge activity inside a thundercloud. When a discharge consists of many high frequency emission sources, such as streamers, that generate currents in random directions, its radiation spectrum peaks in the HF and VHF bands, and the spectral magnitudes in low frequencies are much smaller or even negligible. Combined with recent observational findings, the present study suggests that lightning initiation may begin with a short burst of many randomly occurring small-scale discharges in a localized thundercloud region.

Thunderstorm high frequency radio bursts with weak low frequency radiation

Ningyu Liu[1], and Joseph R. Dwyer[1]

[1]Department of Physics and Astronomy & Space Science Center (EOS), University of New Hampshire, Durham, New Hampshire, USA, 03824

Key Points:

- A theory is developed to understand the generation mechanism of thunderstorm high frequency radio bursts with weak low frequency radiation
- Many high frequency radio emitting streamers or streamer-like discharges that propagate in random directions can generate such radio bursts
- Lightning initiation may begin with a short burst of many randomly occurring small-scale discharges in a localized thundercloud region

Corresponding author: Ningyu Liu, Ningyu.Liu@unh.edu

Abstract

Brief bursts of high frequency (HF) and very high frequency (VHF) radio emissions unaccompanied by strong low frequency radiation have been observed during initiation and propagation of lightning or thunderstorm electrical breakdown without leading to fully-fledged lightning. This paper investigates a physical mechanism to generate such radio bursts by electrical discharge activity inside a thundercloud. When a discharge consists of many high frequency emission sources, such as streamers, that generate currents in random directions, its radiation spectrum peaks in the HF and VHF bands, and the spectral magnitudes in low frequencies are much smaller or even negligible. Combined with recent observational findings, the present study suggests that lightning initiation may begin with a short burst of many randomly occurring small-scale discharges in a localized thundercloud region.

Plain Language Summary

How exactly lightning forms from electrical breakdown activity inside thunderclouds remains unclear. To answer this question, radio frequency (RF) radiation originating from thunderstorms is routinely measured and analyzed to investigate lightning dynamics. Recent multi-channel radio observations clearly indicate that brief bursts of high frequency RF radiation unaccompanied by lower frequency waves can be generated during lightning formation. Such radio bursts have different spectral properties than well-documented RF radiation from lightning. This paper investigates a way for electrical breakdown activity to generate such radio bursts. We find those radio bursts can be generated by an electrical discharge consisting of a large number of elements that propagate in random directions. Our finding suggests that lightning may begin with many randomly occurring small-scale electrical discharges in a localized thundercloud volume.

1 Introduction

A variety of lightning processes generate broadband radio frequency (RF) emissions. The spectrum of the RF radiation typically peaks around 5-10 kHz in the very low frequency (VLF, 3-30 kHz) range and rolls off above approximately 10 MHz (e.g., Willett et al., 1990). A notable exception is the spectrum of compact intra-cloud discharges (CIDs) or narrow bipolar events (NBEs), which has elevated magnitude in high frequency (HF, 3-30 MHz) and very high frequency (VHF, 30-300 MHz) bands (e.g., Le Vine, 1980; Willett et al., 1989; Smith et al., 1999; Jacobson et al., 1999). However, even for CIDs the spectral magnitude in the high frequency range is still much smaller than that of lower frequencies (e.g., Willett et al., 1989; Liu et al., 2019).

Recent multi-band radio observations have clearly shown that bursts of HF and VHF radiation with only weak or even no accompanying sferic pulses (i.e., weak lower frequency radiation) can also be generated during thunderstorms. Examples of such RF bursts include the microsecond-long radiation from the initial breakdown of precursor events reported by Rison et al. (2016), which are thundercloud discharges not leading to fully-fledged lightning, and narrow (e.g., $\leq$0.5 μs) VHF pulses that are the initiating events of a large fraction of lightning (Marshall et al., 2019; Lyu et al., 2019) and that also occur during lightning formation (Marshall et al., 2019). Interestingly, long-lasting ($\sim$1 s) bursts of VHF radiation called continual radio frequency (CRF) have been observed during the onset of explosive volcanic eruptions (e.g., Behnke et al., 2018; Thomas et al., 2007). Radio observations indicate that CRF consists of fast ($\sim$160 ns) VHF impulses that occur on average once every faction of a millisecond, is produced in the absence of a large-scale electric field, and results in insignificant charge transfer (Behnke et al., 2013, 2018). Behnke et al. (2018) has suggested that CRF is caused by numerous, small electrical discharges similar to streamers.

The purpose of the present study is to investigate a physical mechanism for production of HF and VHF bursts without significant lower frequency radiation. The dominant source of lightning high frequency radiation has been referred to by a loosely defined term, dielectric breakdown in virgin air. Recent studies have narrowed it down to streamer discharges (Rison et al., 2016; Shi et al., 2016, 2019; Tilles et al., 2019; Liu et al., 2019). A streamer under certain ambient field conditions can quickly expand and accelerate, resulting in a rapidly increasing current with a growth timescale on the order of nanoseconds. As shown by recent studies (Liu et al., 2019, 2020; Cooray et al., 2020), a large ensemble of streamers that all propagate in the same direction can explain the elevated spectral magnitude in the HF and VHF bands such as the spectrum of CIDs. This is because as the streamers randomly occur over a time interval (e.g., the duration of the CIDs) much longer than their growth timescale, the radio spectral properties of individual streamers that are related to their growth timescale will still be manifested due to the random onset of the streamers. Another way to understand the CID spectrum is that as the electromagnetic fields of individual streamers are added together to give the field of the CID, the lower frequency components (on the order of the inverse of the CID duration) are added coherently, but the high frequency components are added incoherently. As a result, although the spectral magnitude in the high frequency range is much smaller than the lower-frequency spectral magnitude, the CID spectrum in this range is as flat as the radiation spectrum of a single streamer. The coherency of the lower frequency components of the radiated fields from individual streamers is imposed by the occurrences of the streamers within the duration of the CID. Then, in order to explain the observed HF-VHF bursts unaccompanied by sferic pulses, the lower frequency components of the radiated fields of individual streamers must cancel out when they are added up coherently in time. This can be achieved if streamer propagation is not constrained to a single direction.

In this paper, we develop the theory of electromagnetic radiation from an ensemble of streamers that occur randomly in time and propagate in random directions. This theory indicates that the intensity of the high frequency radiation from such a system is comparable to that from an ensemble of streamers that all propagate in a single direction, but the radiation intensity is weak in lower frequencies and is in fact negligible near zero frequencies. Numerical simulations are also presented to validate the developed theory. Combined with the observation of lightning initiated by a narrow VHF pulse (Marshall et al., 2019; Lyu et al., 2019), the results from this study suggest lightning initiation may begin with many small-scale discharges between charged particles that randomly occur in a relatively localized thunderstorm volume.

2 Theory

The radiated electric field from a time-varying current can be calculated by the following equation (e.g., McDonald, 1997; Shao, 2016):

$$\vec{E}_{rad}(\vec{r},t) = \frac{1}{4\pi\varepsilon_0}\int \frac{\left\{\dot{\vec{J}}(\vec{r'}, t-R/c)\times\hat{R}\right\}\times\hat{R}}{c^2 R}d\tau' = -\frac{1}{4\pi\varepsilon_0}\int \frac{\left[\dot{\vec{J}}\right] - \left(\left[\dot{\vec{J}}\right]\cdot\hat{R}\right)\hat{R}}{c^2 R}d\tau',$$

where ε_0 is the permittivity of free space, c is the speed of light, $\hat{R}$ is the unit vector of the separation vector $\vec{R}$ from the source point $\vec{r'}$ to the observation point $\vec{r}$, and $\dot{\vec{J}}$ is the time derivative of the current density. The square brackets surrounding $\dot{\vec{J}}$ means the current density is evaluated at the retarded time $t-R/c$. Note that the numerator of the last integral gives the component of $\dot{\vec{J}}$ in the direction perpendicular to $\hat{R}$ and the negative sign in front of the integral indicates that the radiated electric field is opposite to the total current moment derivative.

As an electric field antenna typically measures a single component of $\vec{E}_{rad}$, without loss of generality, we consider the z component:

$$E_z(\vec{r},t) = \vec{E}_{rad} \cdot \hat{z} = -\frac{1}{4\pi\varepsilon_0} \int \frac{\left[\dot{\vec{J}}\right] \cdot \hat{z} - \left(\left[\dot{\vec{J}}\right] \cdot \hat{R}\right)\left(\hat{R} \cdot \hat{z}\right)}{c^2 R} d\tau'.$$

The duration of the HF and VHF bursts considered here is very short, at most a couple of microseconds, suggesting that the source volume must be small. Setting the origin of the coordinates at the center of the volume and neglecting the variation of $\vec{R}$ except for evaluating $\dot{\vec{J}}$ at the retarded time, the following equation is obtained, with $\hat{z} = \cos\theta\hat{R} - \sin\theta\hat{\theta}$ and $\hat{R} \cdot \hat{z} = \cos\theta$:

$$E_z(\vec{r},t) = \frac{\sin\theta}{4\pi\varepsilon_0 c^2 R} \left(\hat{\theta} \cdot \int \left[\dot{\vec{J}}\right] d\tau'\right).$$

That is to say, to find E_z, we can first calculate the θ component of the total current moment derivative, and then find the projection of the result onto the z axis. If a different component of $\vec{E}_{rad}$ is wanted, we just need to replace θ and $\hat{\theta}$ with the corresponding quantities for that component.

For an ensemble of discrete streamers, each streamer generates a current moment pulse and so an electric field pulse (Liu et al., 2019, 2020). The above equation can then be written as

$$E_z(\vec{r},t) = \frac{\sin\theta}{4\pi\varepsilon_0 c^2 R} \left(\hat{\theta} \cdot \sum_i \left[\dot{\vec{M}}_i\right]\right),$$

where $\left[\dot{\vec{M}}_i\right] = \dot{\vec{M}}_i(t - R_i/c)$ is the time derivative of the current moment of the ith streamer evaluated at the retarded time. Let $\vec{M}_i = M_s(t-t_i)\hat{n}_i$, where $M_s(t)$ is a reference streamer current moment waveform (Liu et al., 2019), t_i is the delay of the start of the ith streamer, and $\hat{n}_i$ is its propagation direction. Introducing $T_i = t_i + R_i/c$, $\left[\dot{\vec{M}}_i\right] = \dot{M}_s(t - t_i - R_i/c)\hat{n}_i = \dot{M}_s(t - T_i)\hat{n}_i$, so T_i is the total delay of the radiated electric field from the ith streamer to arrive at the observation point. Taking Fourier transform of E_z, we obtain

$$\tilde{E}_z(\vec{r},t) = \frac{\omega\tilde{M}_s \sin\theta}{4\pi\varepsilon_0 c^2 R} \left(\hat{\theta} \cdot \sum_i e^{-j\omega T_i}\hat{n}_i\right).$$

Because of the random nature of streamer occurrence, the electromagnetic radiation spectrum of a streamer ensemble contains strong fluctuations and the essential information can be found in the average spectrum of streamer ensembles (Dwyer & Cummer, 2013; Liu et al., 2019, 2020). As the energy spectral density (ESD) of the radiated field is proportional to $|\tilde{E}|^2$ (Liu et al., 2019; Shi et al., 2019), we need to compute $\left\langle |\tilde{E}_z|^2 \right\rangle$. With $\tilde{E}_z = \left\langle \tilde{E}_z \right\rangle + d\tilde{E}_z$, where $\left\langle \tilde{E}_z \right\rangle$ is the average and $d\tilde{E}_z$ is the deviation of a streamer ensemble from the average,

$$\left\langle |\tilde{E}_z|^2 \right\rangle = \left|\left\langle \tilde{E}_z \right\rangle\right|^2 + \left\langle |d\tilde{E}_z|^2 \right\rangle,$$

under the assumption that $\left\langle < \tilde{E}_z > d\tilde{E}_z^* \right\rangle = \left\langle < \tilde{E}_z^* > d\tilde{E}_z \right\rangle = 0$.

Suppose that T_i follows certain probability distribution $f_{\text{ens}}(t')$, and $\hat{n}_i$ is equally probably to point to any direction denoted by $\hat{r}(\theta', \phi')$ so that the corresponding probability distribution $f_d(\theta', \phi')$ is given by $\sin\theta'/4\pi$, where primed coordinates represent the quantities of the source. Then,

$$\left\langle \tilde{E}_z(\vec{r},t) \right\rangle = \frac{\omega \tilde{M}_s \sin\theta}{4\pi\varepsilon_0 c^2 R}\hat{\theta}\cdot\left\langle \sum_i e^{-j\omega T_i}\hat{n}_i \right\rangle = \frac{\omega \tilde{M}_s \sin\theta}{4\pi\varepsilon_0 c^2 R}\hat{\theta}\cdot\sum_k\sum_l\sum_m e^{-j\omega T_k}\hat{r}(\theta'_l,\phi'_m)\left\langle N_{k,l,m}\right\rangle$$
$$= \frac{\omega \tilde{M}_s \sin\theta}{4\pi\varepsilon_0 c^2 R}\hat{\theta}\cdot\int_0^T\int_0^\pi\int_0^{2\pi} e^{-j\omega t'}\hat{r}(\theta',\phi')Nf_{\text{ens}}(t')f_d(\theta',\phi')dt'd\theta'd\phi',$$

where N is the total number of streamers in the ensemble and $N_{k,l,m}$ is the number of streamers with a delay of T_k and propagating in the $r(\theta'_l,\phi'_m)$ direction. With $\hat{r}=\sin\theta'\cos\phi'\hat{x}+\sin\theta'\sin\phi'\hat{y}+\cos\theta'\hat{z}$ and $\langle\cos\phi'\rangle = \langle\sin\phi'\rangle = \langle\cos\theta'\rangle = 0$ for the assumed angular distribution $f_d(\theta',\phi')=\sin\theta'/4\pi$,

$$\left\langle \tilde{E}_z(\vec{r},t) \right\rangle = 0,$$

and

$$\left\langle |\tilde{E}_z|^2 \right\rangle = \left\langle |d\tilde{E}_z|^2 \right\rangle.$$

Because $d\tilde{E}_z$ arises from fluctuation of the number of streamers that start at a particular moment of time and propagate in certain direction from the average number,

$$d\tilde{E}_z = \frac{\omega \tilde{M}_s \sin\theta}{4\pi\varepsilon_0 c^2 R}\hat{\theta}\cdot\sum_k\sum_l\sum_m e^{-j\omega T_k}\hat{r}(\theta'_l,\phi'_m)dN_{k,l,m}.$$

With $\left\langle |d\tilde{E}_z|^2 \right\rangle = \left\langle d\tilde{E}_z d\tilde{E}_z^* \right\rangle$, we have

$$\left\langle |d\tilde{E}_z|^2 \right\rangle = \frac{\sin^2\theta\omega^2|\tilde{M}_s|^2}{(4\pi\varepsilon_0 c^2 R)^2}\sum_k\sum_l\sum_m\sum_{k'}\sum_{l'}\sum_{m'} e^{-j\omega(T_k-T_{k'})}\left(\hat{\theta}\cdot\hat{r}(\theta'_l,\phi'_m)\right)\left(\hat{\theta}\cdot\hat{r}(\theta'_{l'},\phi'_{m'})\right)\left\langle dN_{k,l,m}dN_{k',l',m'}\right\rangle$$

Assuming $\langle dN_{k,l,m}dN_{k',l',m'}\rangle \neq 0$ only if $k=k'$, $l=l'$, and $m=m'$,

$$\left\langle |d\tilde{E}_z|^2 \right\rangle = \frac{\sin^2\theta\omega^2|\tilde{M}_s|^2}{(4\pi\varepsilon_0 c^2 R)^2}\sum_k\sum_l\sum_m\left(\hat{\theta}\cdot\hat{r}(\theta'_l,\phi'_m)\right)^2\left\langle dN^2_{k,l,m}\right\rangle = \frac{\sin^2\theta\omega^2|\tilde{M}_s|^2}{(4\pi\varepsilon_0 c^2 R)^2}\sum_k\sum_l\sum_m\left(\hat{\theta}\cdot\hat{r}(\theta'_l,\phi'_m)\right)^2\left\langle N_{k,l,m}\right\rangle$$
$$= \frac{\sin^2\theta\omega^2|\tilde{M}_s|^2}{(4\pi\varepsilon_0 c^2 R)^2}\int_0^T\int_0^\pi\int_0^{2\pi}\left(\hat{\theta}\cdot\hat{r}(\theta',\phi')\right)^2 Nf_{\text{ens}}(t')f_d(\theta',\phi')dt'd\theta'd\phi',$$

where $\left\langle dN^2_{k,l,m}\right\rangle = \langle N_{k,l,m}\rangle$ is used because $N_{k,l,m}$ follows Poisson distribution.

As $\hat{r}$ follows an isotropic distribution, without loss of generality, we can set $\hat{\theta} = \hat{z}$ to compute the above integral so that $\left(\hat{\theta}\cdot\hat{r}(\theta',\phi')\right) = \cos\theta'$. Because $\int_0^T f_{\text{ens}}(t')dt' = 1$, $f_d(\theta',\phi')=\sin\theta'/4\pi$, and $\int_0^\pi\int_0^{2\pi}\cos^2\theta'\sin\theta'/(4\pi)d\theta'd\phi' = 1/3$,

$$\left\langle |\tilde{E}_z|^2 \right\rangle = \left\langle |d\tilde{E}_z|^2 \right\rangle = \frac{\sin^2\theta\omega^2|\tilde{M}_s|^2}{48\pi^2\varepsilon_0^2 c^4 R^2}N. \tag{1}$$

This equation means that $\left\langle |\tilde{E}_z|^2 \right\rangle$ is proportional to $\omega^2|\tilde{M}_s|^2$, which is the squared magnitude of the Fourier transform of the derivative of a single streamer current moment pulse. It also shows that $\left\langle |\tilde{E}_z|^2 \right\rangle$ is linearly proportional to the total number of streamers. Because each streamer produces a brief current pulse, $|\tilde{M}_s|^2$ is constant over low frequencies so that the energy spectral density increases with frequency in that frequency range. As the frequency increases further, the timescales of streamer current first compensate the ω^2 term, giving a constant energy spectral density in the HF and VHF range, and then further lead to decreasing energy spectral density with increasing frequency. Compared to the case of streamers propagating in the same direction (Liu et al., 2019), the HF-VHF power is a factor of three smaller.

3 Numerical Simulation

To validate the theory presented above, numerical simulations are performed to obtain the electromagnetic radiation spectrum of an ensemble of streamers propagating in random directions. The currents from the streamers are added together to obtain the total current of the ensemble and then Fourier transform is performed on the time derivative of the total current in order to obtain the energy spectral density. Starting from $E_z(\vec{r},t)$, with $\left[\dot{\vec{M}}_i\right] = \dot{M}_s(t-T_i)\vec{n}_i$, we have

$$E_z(\vec{r},t) = \frac{\sin\theta}{4\pi\varepsilon_0 c^2 R}\sum_i \dot{M}_s(t-T_i)\left(\hat{\theta}\cdot\vec{n}_i\right),$$

Again, $\left(\hat{\theta}\cdot\vec{n}_i\right) = \cos\theta'$. Then,

$$E_z(\vec{r},t) = \frac{\sin\theta}{4\pi\varepsilon_0 c^2 R}\sum_i \dot{M}_s(t-T_i)\cos\theta_i'.$$

If the number of streamers N in the ensemble is not too large, the summation over all streamers in the above equation can be readily implemented in numerical simulation to find $E_z(\vec{r},t)$, with T_i and θ_i' drawn from $f_{\text{ens}}(t)$ and $\sin\theta/2$ distributions, respectively.

If N is large, the following manipulations are made in order to improve the performance of the simulation. Dividing the duration of the event into small intervals of ΔT and the $[0,\,\pi]$ range of θ' into small segments of $\Delta\theta'$, and introducing $N_{k,l}$ as the number of streamers starting at $t=T_k$ and propagating along the direction $\theta'=\theta_l'$,

$$E_z(\vec{r},t) = \frac{\sin\theta}{4\pi\varepsilon_0 c^2 R}\sum_k\sum_l \dot{M}_s(t-T_k)\cos\theta_l' N_{k,l}, \tag{2}$$

with

$$\langle N_{k,l}\rangle = N f_{\text{ens}}(T_k)\frac{\sin\theta_l'}{2}\Delta T\Delta\theta'.$$

Equation (2) is then implemented with $N_{k,l}$ drawn from a Poisson distribution with the mean given above. The simulations shown below are obtained with this approach.

4 Simulation Results

In simulation, $f_{\text{ens}}(t)$ is assumed to be an asymmetric two-sided exponential (Liu et al., 2019):

$$f_{\text{ens}}(t) = \frac{a_e b_e}{a_e+b_e}[e^{a_e(t-t_0)}u(t_0-t)+e^{-b_e(t-t_0)}u(t-t_0)], \tag{3}$$

where a_e and b_e are the inverses of the rise and fall time constants, respectively, $u(t)$ is the step function, and t_0 is the time when $f_{\text{ens}}(t)$ reaches its peak. The streamer current moment pulse is assumed to be described by a double exponential function (Liu et al., 2019):

$$M_s(t) = \frac{M_{s0}e^{a_s t}}{1+e^{(a_s+b_s)t}}, \tag{4}$$

where a_s and b_s are the growth and decay rates, respectively, and M_{s0} is approximately the peak current moment. Two simulation cases are reported below, and the parameters used are summarized in Table 1. Equation (2) indicates that E_z depends on both R and θ, but equation (1) shows the spectral shape is independent from those two quantities. For simplicity, θ is set to $\pi/2$, the direction where the spectral magnitude is maximized, and R is set to 100 km, the distance the radiated field from lightning is typically normalized to.

Table 1. Parameters for the two simulation cases.

Case	N	a_e^{-1} (μs)	b_e^{-1} (μs)	Duration[a] (μs)	a_s^{-1} (ns)	b_s^{-1} (μs)	M_{s0} (A-m)	θ (rad)	R (km)
1	10^5	0.5	1	1.5	1	0.25	1.0	$\pi/2$	100
2	10^3	0.125	0.25	0.375	1	0.125	1.0	$\pi/2$	100

[a]Calculated as $(a_e^{-1} + b_e^{-1})$.

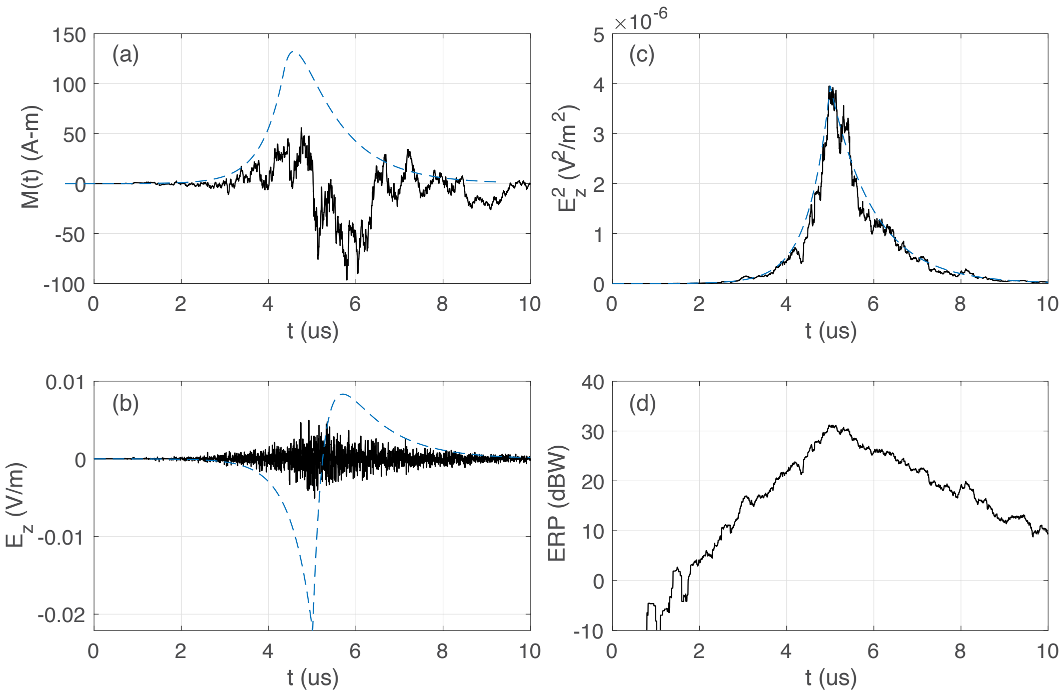

Figure 1. Simulation results of an ensemble of 10^5 streamers that occur randomly in a time interval of about 1.5 μs and propagate in random directions. a) The simulated current moment (solid line) and the current moment (reduced by factor of 100 in plotting) of a streamer system without any random fluctuations (dashed line). b) The electric field at 100 km calculated by the current moments shown in a). c) The square (solid line) of the rms envelope of E_z smoothed over a 0.2 μs window and $f_{ens}(t)$ (dashed line) that is scaled to the same peak as the black curve. d) The effective radiated power (ERP) in dBW.

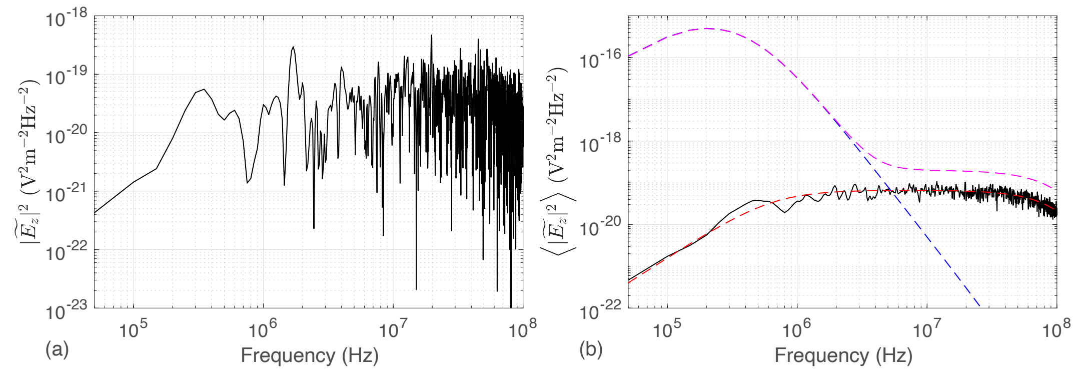

Figure 2. The energy spectral density of an ensemble of 10^5 streamers that occur randomly in a time interval of about 1.5 μs and propagate in random directions. a) The ESD of a single ensemble of 10^5 streamers. b) The ESDs obtained from averaging over 20 simulated streamer ensembles (solid black curve), equation (1) (dashed red curve), theoretical mean (dashed magenta curve) of ensembles of streamers all propagating in the same direction, and a system of streamers without any random fluctuations (dashed blue curve).

Figure 1 presents the waveforms of several quantities from the first simulation case. The solid line in panel 1a shows the current moment component relevant to E_z, i.e., $\sum_k \sum_l M_s(t-T_k)\cos\theta_l' N_{k,l}$ (see equation (2)). The dashed line is the result (reduced by a factor 100) of convolving the streamer current with $f_{\rm ens}(t)$, which can be thought as the total current moment if all streamers propagate in the same direction and if there is no random fluctuation in the streamer onset (Liu et al., 2019). Because of the cancellation due to random directions of the streamer currents, the peak magnitude of the solid black curve is about two orders of magnitude smaller than that of the dashed blue line. The total charge moment change from the dashed blue line is 25 mC-m, consistent with 10^5 streamers each with a charge moment change of 0.25 μC-m, while the total charge moment change from the black curve is much smaller, with a value of -44 μC-m. More importantly, the current moment shown by the solid black curve is not exactly zero and varies rapidly. As a result, the electric field E_z, shown by the solid black curve in panel 1b, calculated by using equation (2) clearly contains high frequency components and its peak magnitude is not significantly smaller than the field for the case with no random fluctuations (the dashed blue line), calculated by multiplying the time derivative of the smooth current moment waveform in panel 1a by $-\sin\theta/(4\pi\varepsilon_0 c^2 R)$. In panel 1c, the solid black line shows the square of the smoothed root mean square (rms) envelope of the simulated electric field E_z, which recovers $f_{\rm ens}(t)$ (the dashed blue line). Panel 1d shows the effective radiated power (ERP) in dBW, which is defined as the total power radiated as if the source is a point source emitting isotropically (Jacobson et al., 2013). The ERP in dBW is calculated as $10\log_{10}[4\pi R^2\varepsilon_0 c E_z^2)]$, where the smoothed envelope shown in panel 1c is used for E_z^2.

The ESD as represented by $|\tilde{E}_z|^2$ is shown in Figure 2. Because the ESD from a single streamer ensemble is also a random process, the simulated ESD obtained by taking Fourier transform of E_z shown in Figure 1b fluctuates greatly, as shown in panel 2a. Panel 2b shows that the average ESD (solid black curve) of 20 simulated streamer ensembles agrees well with the spectrum predicted by equation (1) (dashed red curve). The ESD increases initially, $\propto \omega^2$, with increasing frequency until it plateaus starting around 1 MHz, and it finally rolls off near 100 MHz. Compared to the ESD of the ensemble of streamers propagating in the same direction, calculated as $[\sin\theta/(4\pi\varepsilon_0 c^2 R)]^2 2N^2\omega^2|\tilde{M}_s|^2(|\tilde{f}_{\rm ens}|^2 + 1/N)$ [see equation (14) in (Liu et al., 2019) and note that the extra factor of 2 takes into

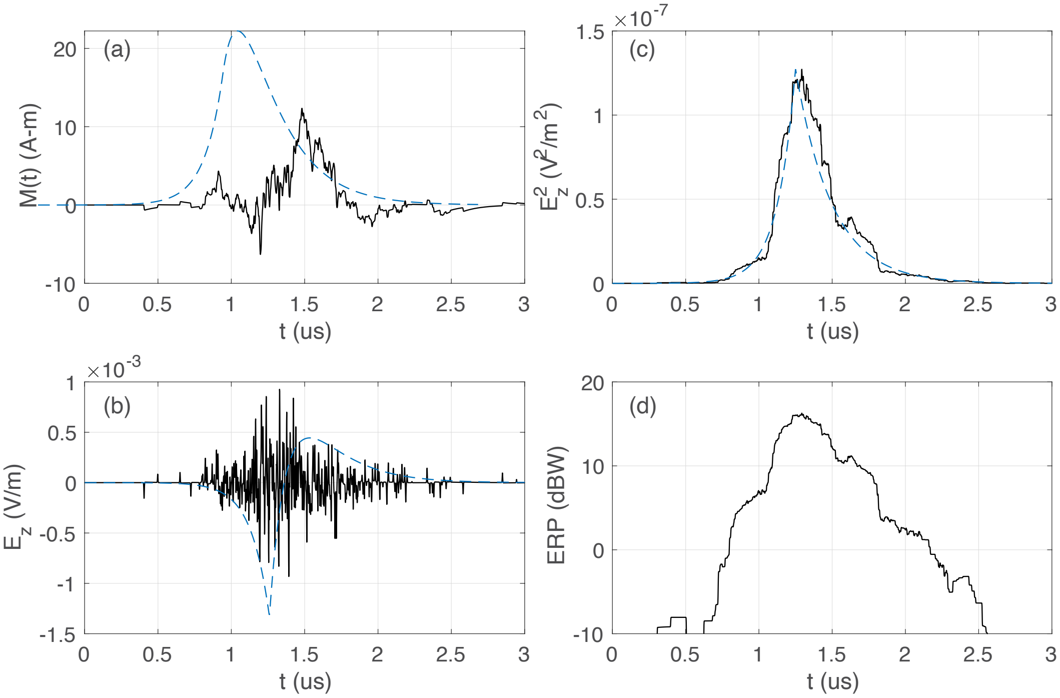

Figure 3. Simulation results of an ensemble of 10^3 streamers that occur randomly in a time interval of about 0.375 μs and propagate in random directions. The description of each panel is the same as Figure 1 except the dashed blue line in panel a) shows the current moment reduced by a factor of 10, instead of 100.

account the negative frequencies.], the ESD in the HF and VHF range is only slightly smaller, a factor of three smaller according to equation (1), but it is more than four orders of magnitude smaller at 100 kHz and even smaller at lower frequencies. The ESD from a streamer ensemble without any fluctuations in the streamer onset and propagation direction matches the ESD of the ensemble of the streamers propagating along a single direction in the low frequency region, but it decreases initially with a power law index of -4 above several hundreds of kHz as it is proportional to $\omega^2|\tilde{M}_s|^2|\tilde{f}_{\mathrm{ens}}|^2$.

Figures 3 and 4 show the simulation results from the second case. The features of the results are consistent with those of Figures 1 and 2. The current moment of the simulated streamer ensemble is significantly smaller than the ensemble with all streamer propagating in the same direction, but the peak magnitude of the electric field is comparable. The electric field is very noisy and the square of the smoothed envelope of E_z matches well with the streamer occurrence probability distribution in time $f_{\mathrm{ens}}(t)$. For the ESD plots, the average ESD from simulated streamer ensembles agrees well with equation (1). It is slightly smaller than the ESD of the system of streamers propagating in the same direction above several MHz, but many orders of magnitude smaller in the low frequency region.

5 Discussion

The key ingredients for generating RF emissions with the particular spectral features considered in this paper are 1) the source consists of many elements and 2) the currents of the elements flow in random directions. For thunderstorm streamers, a simple field configuration for them to propagate in random directions is a localized strong field

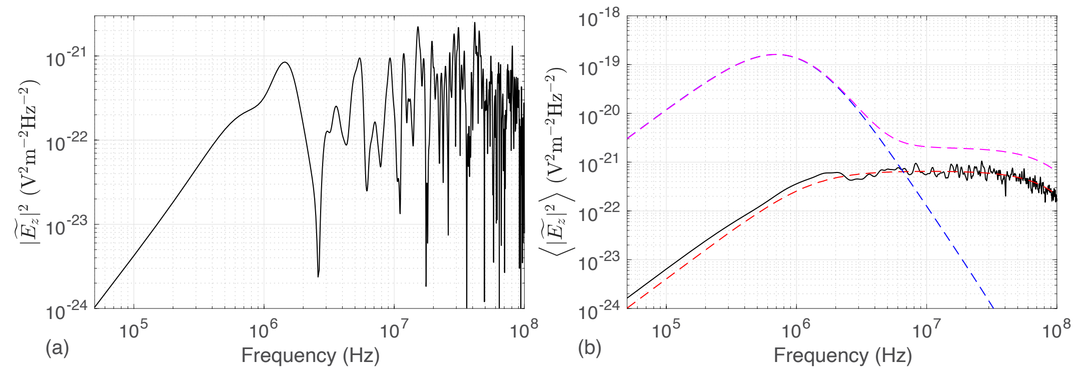

Figure 4. The energy spectral density of an ensemble of 10^3 streamers that occur randomly in a time interval of about 0.375 μs and propagate in random directions. See the caption of Figure 2 for the description of each panel.

region with the field either diverging or converging to the center. Consider a uniformly charged spherical thundercloud volume with a radius of a. In order to not only initiate streamers but also ensure that the streamer current moment increases on a short enough timescale of a few nanoseconds to emit VHF radiation (Shi et al., 2016), the maximum electric field in this region needs to reach $0.5E_k$, where the conventional breakdown threshold field of air E_k scales with air density and has a value of 3.2×10^6 V/m at ground pressure. If the maximum field of the uniformly charged sphere, which is located at the boundary of the volume, is equal to $0.5E_k$, the total amount of charge in the volume is $Q = 2\pi\varepsilon_0 a^2 E_k$ with a charge density of $\rho = 3\varepsilon_0 E_k/(2a)$. As the thunderstorm VHF bursts without strong sferics typically last $<\sim 2$ μs, the size of the this region should be on the order of 100 m because the fastest speed of breakdown in virgin air is on the order of 5×10^7 m/s (Rison et al., 2016; Tilles et al., 2019). If a is set to 100 m and the altitude under consideration is about 6 km (E_k is reduced to half of its ground value), the required charge density is over 30 times larger than the maximum thundercloud charge density of $\rho_m = +6.7$ nC/m^3 found by Marshall and Stolzenburg (1998). Or the total amount of charge in a spherical volume of about 300 m radius with a density of 6.7 nC/m^3 has to be packed into a sphere of 100 m radius. This might be possible due to turbulence but is unlikely during non-turbulent thunderstorm conditions because a large number of cloud particles are involved. For smaller values of a, the required charged density is even higher, and it may be even more unlikely.

Marshall and Stolzenburg (1998) also found that the maximum cloud charge density of $+6.7$ nC/m^3 was located just above the main negative charge region, and the coexisting precipitation charge of negative polarity in this region reaches a slightly smaller density magnitude of 6.5 nC/m^3. The charged particles are well mixed and the net charge density is approximately zero. It is entirely possible that discharges randomly occur between the charged particles of opposite polarities. According to the study of positive corona inception from spherical hydrometeors (Liu et al., 2012), the threshold charge required on a hydrometeor to initiate a self-sustaining positive corona discharge is very close to the maximum precipitation charge that has been measured. The required amount of charge decreases with increasing altitude for a hydrometeor with a fixed size. At 6 km altitude, 590 pC is required to initiate corona discharges on a hydrometeor of 1 mm radius. If the radius of the hydrometeor is smaller, the required amount of charge will also be smaller. The maximum precipitation charge found from measurements is over 400 pC (MacGorman & Rust, 1998, p. 186, and references cited therein), and the corona discharge is likely responsible for setting the limit of the precipitation charge (Liu et al., 2012). The theory developed in this paper also applies to an ensemble of corona discharges as long as the shortest timescale of their current variation is on the order of a few nanoseconds so that VHF emissions are produced. Note that streamer formation in general requires more intense avalanche multiplication than self-sustaining corona discharges. This requires a stronger electric field between the charged particles, which can be achieved with more charge residing on the charged particles and/or the presence of a non-negligible ambient thundercloud field. In addition, the discharges between two approaching hydrometeors as studied in (Cai et al., 2017, 2018; Jánský & Pasko, 2020) may be particularly relevant. In any case, it seems that small-scale discharges between charged particles are likely to be the source of the VHF bursts. These small discharges randomly occur in a localized region on the order of 100 m or smaller and produce rapid variation of currents although collectively resulting in a negligible charge transfer. In order for many these discharges to occur in a short time period of microseconds or less, it seems a cascade of these small-scale discharges triggered by a single event is necessary. The triggering event causes discharges in the immediate surrounding region, and then their effects ripple through a region of tens of meters or hundreds of meters to cause more discharges between particles.

Regarding CRF observed during the onset of explosive volcanic eruptions, Behnke et al. (2018) have concluded that it originates from the gas thrust region of the eruption column, which is characterized by higher particle density and turbulence. In addition, it is believed that charge is well mixed in the eruption column as no significant electric field change was observed. The VHF impulses constituting CRF occur at a rate of several thousands to over 10,000 impulses per second, but no significant charge transfer is detected during second-long CRF. Behnke et al. (2018) have suggested that the more likely sources of CRF are small streamer-like discharges between small pockets of charge or individual charged particles. Our study supports their conclusions and in addition, suggests that those discharges must generate currents that flow in random directions.

Acknowledgments
We thank Abe Jacobson, Martin Füllekrug, and Steve Cummer for useful discussions on lightning radio emissions. This research was supported in part by AFOSR Grants No. FA9550-18-1-0358 and No. FA9550-16-1-0396, and NSF Grant No. AGS-1552177 to the University of New Hampshire. Disclaimer: the views expressed are not endorsed by the sponsors. The simulation data plotted are available at: `https://doi.org/10.6084/m9.figshare.12794567.v1`

References

Behnke, S. A., Edens, H. E., Thomas, R. J., Smith, C. M., McNutt, S. R., Van Eaton, A. R., ... Cigala, V. (2018, April). Investigating the origin of continual radio frequency impulses during explosive volcanic eruptions. *J. Geophys. Res. Atmos.*, *123*(8), 4157-4174. doi: 10.1002/2017JD027990

Behnke, S. A., Thomas, R. J., McNutt, S. R., Schneider, D. J., Krehbiel, P. R., Rison, W., & Edens, H. E. (2013, June). Observations of volcanic lightning during the 2009 eruption of Redoubt Volcano. *J. Volcanol. Geotherm. Res*, *259*, 214-234. doi: 10.1016/j.jvolgeores.2011.12.010

Cai, Q., Jánskỳ, J., & Pasko, V. P. (2017). Initiation of positive streamer corona in low thundercloud fields. *Geophys. Res. Lett.*, *44*(11), 5758–5765.

Cai, Q., Jánskỳ, J., & Pasko, V. P. (2018, July). Initiation of streamers due to hydrometeor collisions in thunderclouds. *J. Geophys. Res. Atmos.*, *123*(14), 7050-7064. doi: 10.1029/2018JD028407

Cooray, V., Cooray, G., Rubinstein, M., & Rachidi, F. (2020, May). Modeling compact intracloud discharge (CID) as a streamer burst. *Atmosphere*, *11*(5), 549. doi: 10.3390/atmos11050549

Dwyer, J. R., & Cummer, S. A. (2013, June). Radio emissions from terrestrial gamma-ray flashes. *J. Geophys. Res.*, *118*, 3769-3790. doi: 10.1002/jgra.50188

Jacobson, A. R., Knox, S. O., Franz, R., & Enemark, D. C. (1999, March). FORTE observations of lightning radio-frequency signatures: Capabilities and basic results. *Radio Sci.*, *34*, 337-354. doi: 10.1029/1998RS900043

Jacobson, A. R., Light, T. E. L., Hamlin, T., & Nemzek, R. (2013, March). Joint radio and optical observations of the most radio-powerful intracloud lightning discharges. *Ann. Geophys.*, *31*(3), 563-580. doi: 10.5194/angeo-31-563-2013

Jánský, J., & Pasko, V. P. (2020, March). Modeling of streamer ignition and propagation in the system of two approaching hydrometeors. *J. Geophys. Res. Atmos.*, *125*(6), e2019JD031337. doi: 10.1029/2019JD031337

Le Vine, D. M. (1980, July). Sources of the strongest RF radiation from lightning. *J. Geophys. Res.*, *85*, 4091-4095. doi: 10.1029/JC085iC07p04091

Liu, N. Y., Dwyer, J. R., & Rassoul, H. K. (2012, May). Effects of pressure and humidity on positive corona inception from thundercloud hydrometeors. *J. Atmos. Solar Terr. Phys.*, *80*, 179-186. doi: 10.1016/j.jastp.2012.01.012

Liu, N. Y., Dwyer, J. R., & Tilles, J. N. (2020, July). Electromagnetic Radiation Spectrum of a Composite System. *Phys. Rev. Lett.*, *125*(2), 025101. doi: 10.1103/PhysRevLett.125.025101

Liu, N. Y., Dwyer, J. R., Tilles, J. N., Stanley, M. A., Krehbiel, P. R., Rison, W., … Wilson, J. G. (2019). Understanding the radio spectrum of narrow bipolar events. *J. Geophys. Res. Atmos.*, *124*, 10134-10153. doi: 10.1029/2019JD030439

Lyu, F., Cummer, S. A., Qin, Z., & Chen, M. (2019, Mar). Lightning initiation processes imaged with very high frequency broadband interferometry. *J. Geophys. Res. Atmos.*, *124*, 2994-3004. doi: 10.1029/2018JD029817

MacGorman, D. R., & Rust, W. D. (1998). *The Electrical Nature of Storms.* New York, NY: Oxford Univ. Press.

Marshall, T. C., Bandara, S., Karunarathne, N., Karunarathne, S., Kolmasova, I., Siedlecki, R., & Stolzenburg, M. (2019, March). A study of lightning flash initiation prior to the first initial breakdown pulse. *Atmos. Res.*, *217*, 10-23. doi: 10.1016/j.atmosres.2018.10.013

Marshall, T. C., & Stolzenburg, M. (1998, August). Estimates of cloud charge densities in thunderstorms. *J. Geophys. Res.*, *103*(D16), 19,769-19,775. doi: 10.1029/98JD01674

McDonald, K. T. (1997, November). The relation between expressions for time-dependent electromagnetic fields given by Jefimenko and by Panofsky and Phillips. *Amer. J. Phys.*, *65*(11), 1074-1076. doi: 10.1119/1.18723

Rison, W., Krehbiel, P. R., Stock, M. G., Edens, H. E., Shao, X.-M., Thomas, R. J., … Zhang, Y. (2016). Observations of narrow bipolar events reveal how lightning is initiated in thunderstorms. *Nat. Commun.*, *7*. doi: 10.1038/ncomms10721

Shao, X.-M. (2016, April). Generalization of the lightning electromagnetic equations of Uman, McLain, and Krider based on Jefimenko equations. *J. Geophys. Res. Atmos.*, *121*(7), 3363-3371. doi: 10.1002/2015JD024717

Shi, F., Liu, N. Y., Dwyer, J. R., & Ihaddadene, K. (2019). VHF and UHF electromagnetic radiation produced by streamers in lightning. *Geophys. Res. Lett.*, *46*, 443-451. doi: 10.1029/2018GL080309

Shi, F., Liu, N. Y., & Rassoul, H. K. (2016). Properties of relatively long streamers initiated from an isolated hydrometeor. *J. Geophys. Res. Atmos.*, *121*, 7284–7295. doi: 10.1002/2015JD024580

Smith, D. A., Shao, X. M., Holden, D. N., Rhodes, C. T., Brook, M., Krehbiel, P. R., … Thomas, R. J. (1999, February). A distinct class of isolated intracloud lightning discharges and their associated radio emissions. *J. Geophys. Res.*, *104*, 4189-4212. doi: 10.1029/1998JD200045

Thomas, R. J., Krehbiel, P. R., Rison, W., Edens, H. E., Aulich, G. D., Winn, W. P., ... Clark, E. (2007, February). Electrical activity during the 2006 Mount St. Augustine volcanic eruptions. *Science*, *315*(5815), 1097. doi: 10.1126/science.1136091

Tilles, J. N., Liu, N. Y., Stanley, M. A., Krehbiel, P. R., Rison, W., Stock, M. G., ... Wilson, J. G. (2019). Fast negative breakdown in thunderstorms. *Nat. Commun.*, *10*. doi: 10.1038/s41467-019-09621-z

Willett, J. C., Bailey, J. C., & Krider, E. P. (1989, November). A class of unusual lightning electric field waveforms with very strong high-frequency radiation. *J. Geophys. Res.*, *94*, 16255-16267. doi: 10.1029/JD094iD13p16255

Willett, J. C., Bailey, J. C., Leteinturier, C., & Krider, E. P. (1990, November). Lightning electromagnetic radiation field spectra in the interval from 0.2 to 20 MHz. *J. Geophys. Res.*, *95*, 20367-20387. doi: 10.1029/JD095iD12p20367